

## Supplementary Methods

**The Ran-binding protein-2 (RanBP2) is an allosteric activator of the conventional kinesin-1 motor protein, KIF5B, in a minimal cell-free system.**

*Kyoung-in Cho,<sup>1</sup> Haiqing Yi,<sup>1</sup> Ria Desai,<sup>1</sup> Arthur R. Hand,<sup>2</sup> Arthur L. Haas<sup>3</sup> and Paulo A. Ferreira\*<sup>1, 4</sup>*

Department of Ophthalmology<sup>1</sup>, Department of Molecular Genetics and Microbiology<sup>4</sup>,  
Duke University Medical Center, Durham, NC 27710

Departments of Craniofacial Sciences and Cell Biology<sup>2</sup>, University of Connecticut,  
Farmington, CT 06030

Department of Biochemistry and Molecular Biology<sup>3</sup>, Louisiana State University Health  
Science Center, New Orleans, LA 70112

### **Expression constructs.**

Full length human KIF5B and its C-terminal fragment KIF5B-C (aa#: 527-936) was tagged with 6x-histidine at C-terminal end and cloned into pDest-550 vector. KIF5B-C protein was expressed in BL21(DE) bacterial cells, and purified with TALON<sup>TM</sup> resin (BD Biosciences Clontech) as described for KIF5B. RBD2-KBD-RBD3 and constructs thereof were expressed, purified and whenever applicable, cleaved from glutathione-S-transferase as described before (Cai et al., 2001). Cells were lysed with a French press (Thermo IEC, Needham Heights, USA). Purified human KIF5B-N (aa#: 1-319) was purchased from Cytoskeleton, Inc.

### **End-point ATPase assays of kinesin-1, KIF5B.**

For relative comparison of the ATPase activities, end-point assays of kinesin ATPase activity were carried out with 50 nM of kinesin, various concentrations of RanBP2 constructs, 300 nM of taxol-stabilized microtubules purified from bovine brain, and 0.3 mM of ATP were mixed in 30ul of KRB buffer (15 mM Piperazine-1,4-bis(2-ethanesulfonic acid) (PIPES), pH 7.0, and 5mM MgCl<sub>2</sub>). Microtubules were from Cytoskeleton, Inc., (Denver). End-point ATPase assays were performed by measuring the amount of P<sub>i</sub> released with CytoPhos reagent (Cytoskeleton, Inc., Denver) upon incubation of the reagents for 5 minutes at 25°C and as described elsewhere (Funk et al., 2004). All data represent the average of three experiments. Two-tailed equal variance *t*-test was performed.

### **Assays of kinetics of activation of KIF5B by RBD2-KBD-RBD3 of RanBP2 and constructs thereof.**

N-KIF5B activity was found to be maximal in the presence of 0.2-0.3 μM of taxol-stabilized microtubules. To study the kinetics of activation (turnover rate, s<sup>-1</sup>) of KIF5B by R<sub>2</sub>KR<sub>3</sub>, the experimental procedure was modified and optimized by employing 0.2 μM of taxol-stabilized microtubules, 2.5 nM of KIF5B, 0.3 mM ATP, and various concentrations of R<sub>2</sub>KR<sub>3</sub> and constructs thereof. Kinetics of the assays were monitored between the time points of 5 and 8 min after addition of ATP. To calculate the linear ATP turnover rate of KIF5B, the number of released phosphate molecules (P<sub>i</sub>) was divided by the number of kinesin molecules and time. The amount of P<sub>i</sub> released by KIF5B alone and by R<sub>2</sub>KR<sub>3</sub> and constructs thereof alone at various concentrations were considered

background ATPase activities, and subtracted from the KIF5B calculated values in the presence of  $R_2KR_3$ . No significant variations were observed among different batches of purified KIF5B. Kinetic values were obtained by non-linear fitting of data using GraphPad (GraphPad Software) and Sigmaplot (Systat).

### **Pull-down of KIF5B and microtubules by GST-RBD2-KBD-RBD3 and GST-RBD2-KBD<sub>Mut</sub>-RBD3.**

Pull-down assays were performed with 300 nM of taxol-stabilized microtubules, 100nM of KIF5B, 1 $\mu$ M of GST-  $R_2KR_3$  or GST-  $R_2K_{Mut}R_3$ , and 500 nM ATP or AMPPNP, in 15 mM Piperazine-1,4-bis(2-ethanesulfonic acid) (PIPES) pH 7.0, containing 5mM  $MgCl_2$ . Glutathione-*S*-sepharose beads (AmershamPharmacia) were incubated with GST-fused constructs for 30-min followed by blocking with 3%BSA in PBS for another 30-min. Then, beads were washed and equilibrated with KRB buffer (50mM PIPES, pH 7.0, 5mM  $MgCl_2$ ), and all remaining reagents of the binding reaction were added and incubated gently on a shaker for 30-min at room temperature. Beads were then precipitated, washed six times in the same incubation buffer and co-precipitates were resolved on SDS-PAGE followed by immunoblot analysis with antibodies against kinesin-1 (H2 monoclonal antibody) and acetylated  $\alpha$ -tubulin (Invitrogen).

### **Rotary shadowing electron microscopy and morphometric analysis.**

KIF5B with and without  $R_2KR_3$  was visualized using the mica sandwich technique (Mould et al., 1985) for rotary shadow electron microscopy. Kinetic reactions were set up with KIF5B (50nM) alone or with  $R_2KR_3$  (1 $\mu$ M) in the absence of microtubules.

Then, 4  $\mu$ l of 50% glycerol was added to 6  $\mu$ l of the kinetic reactions in 15 mM PIPES, pH 7.0, 5mM MgCl<sub>2</sub>, to achieve final concentrations of 20% glycerol and 30 nM KIF5B. Five microliters of the KIF5B/glycerol mixture was placed on the surface of a 20 mm square piece of freshly cleaved mica, and the corresponding piece of mica was placed on top, causing the KIF5B/glycerol solution to spread between the two mica sheets. Ten minutes later, the mica sheets were separated and placed on the rotary stage of a Denton DV-502 vacuum evaporator (Denton Vacuum, Moorestown, NJ). After drying under vacuum for about 50 minutes, the samples were rotary shadowed with tungsten at an angle of about 8°, then stabilized by coating with carbon. The replicas were floated off the mica onto distilled water and picked up on 400 mesh copper grids. The specimens were examined and photographed at 52,000x in a Philips CM10 transmission electron microscope (Philips, Eindhoven, The Netherlands) operating at 80 kV. The negatives were scanned at 1200 pixels per inch in an Epson Perfection V750 Pro scanner (Epson, Long Beach, CA), and levels and contrast of the images were adjusted in Adobe Photoshop CS2 (version 9.0.2). The lengths or diameters of the KIF5B molecules were measured with the public domain software ImageJ (version 1.38x), and histograms were constructed using the graphing features in Microsoft Excel 2004 (version 11.3.7).

#### **Supplementary references.**

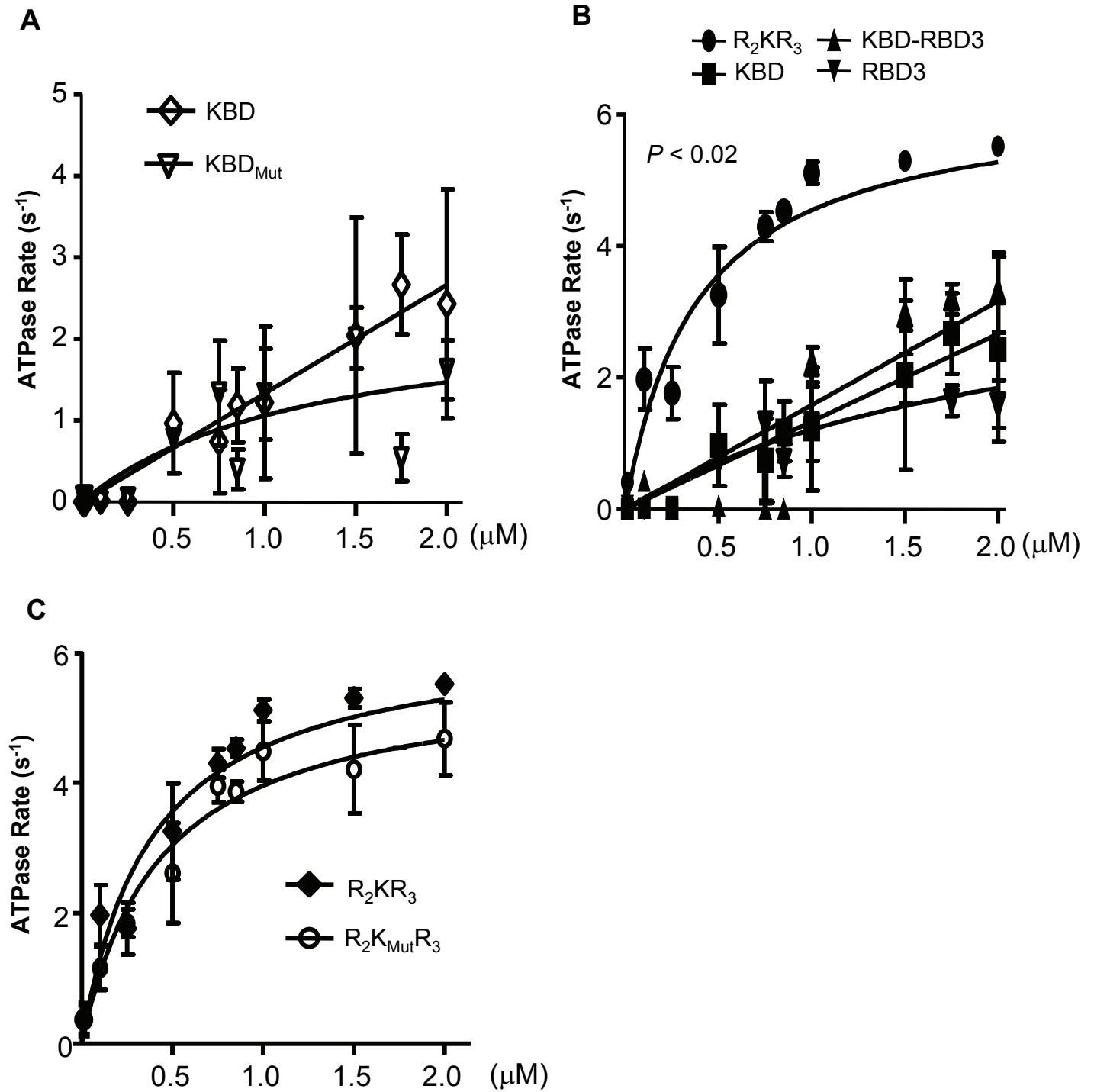
Mould PA, Holmes DF, Kadler KE, Chapman JA (1985). Mica sandwich technique for preparing macromolecules for rotary shadowing. *J Ultrastruct Res* 91:66-76.

## Legends to Supplementary Figures

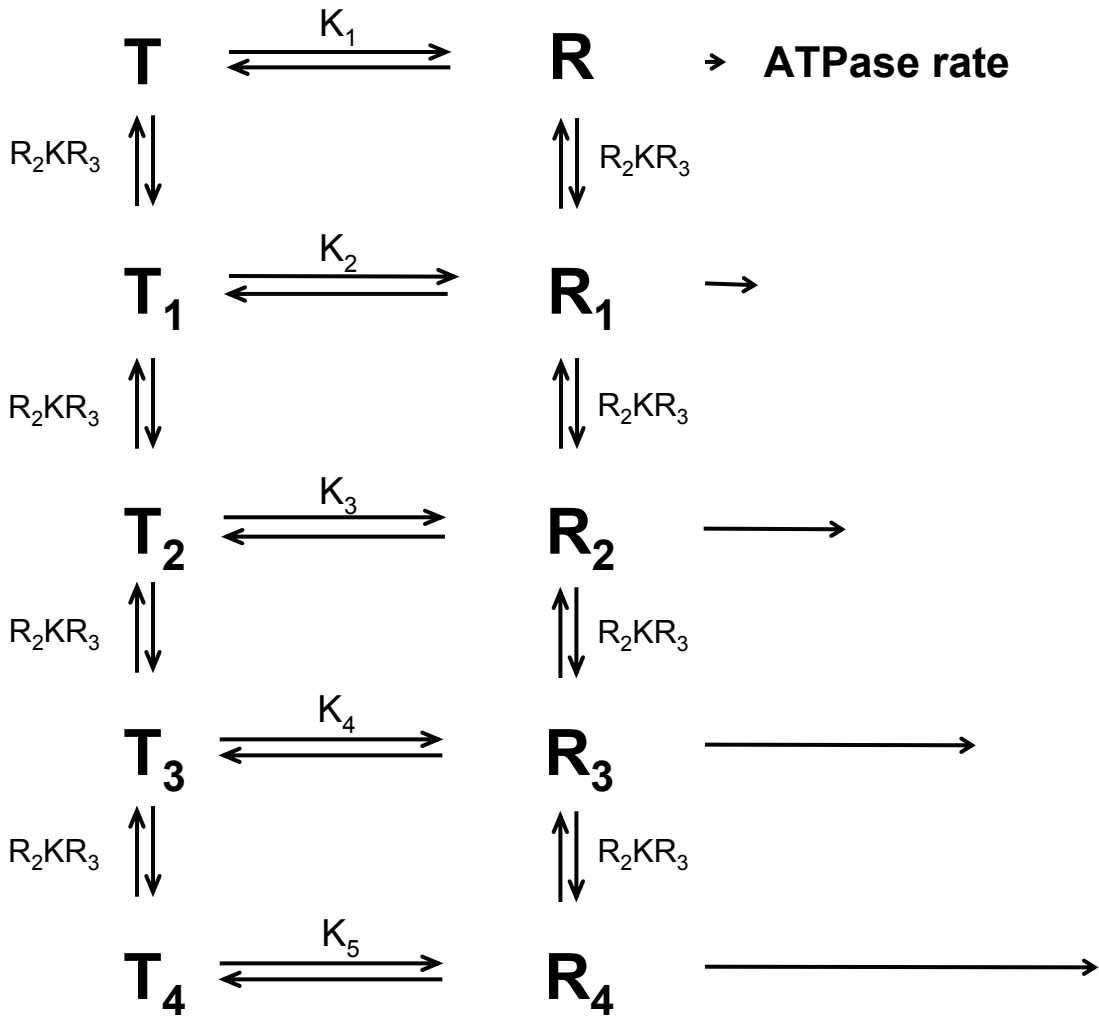
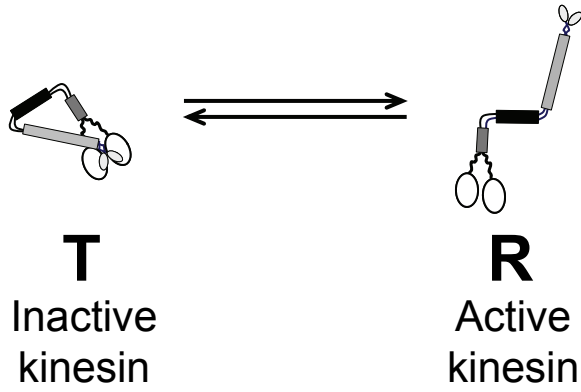
**Supplementary Figure 1.** Analyses of the activation kinetics of KIF5B by the RBD2-KBD-RBD3 ( $R_2KR_3$ ) and domains thereof in the absence of microtubules. **(A)** KIF5B (2.5 nM) does not exhibit specific ATPase activity by KBD and  $KBD_{Mut}$ . **(B)** There is a significant but modest activation of the ATPase rate of the KIF5B (2.5 nM) by  $R_2KR_3$ , whereas other constructs do not present specific ATPase activity. **(C)** A mutation in KBD of  $R_2KR_3$ ,  $R_2K_{Mut}R_3$ , does not affect significantly the modest activation of KIF5B (2.5 nM). Data are means of three independent experiments  $\pm$  standard deviation.

### **Supplementary Figure 2.**

Kinetic model for  $R_2KR_3$ -dependent KIF5B cooperativity. The minimum kinetic model for kinesin cooperativity consistent with the initial rate data assumes that KIF5B exists in two conformations in equilibrium. In the inactive T state, the tail domains bind to the head domain(s), blocking the intrinsic ATPase activity of the latter. Dissociation of the tail from the head domain(s) results in activation of the head domains. The tripartite  $R_2KR_3$  domain of RANBP2 acts as an allosteric activator by promoting dissociation of the tail domain from the kinesin head domain. As an allosteric activator, the  $R_2KR_3$  domain has greater affinity for the R state than for the T state. In the absence of the allosteric activator, the conformational equilibrium ( $K_1$ ) favors the T state. Successive binding of  $R_2KR_3$  shifts the  $T \rightleftharpoons R$  equilibrium toward the R state. The R state exhibits a greater intrinsic ATPase activity than the T state, resulting in increased activity upon  $R_2KR_3$  binding.



Supplementary Figure 1



Supplementary Figure 2